

8 Polymer-based models of cytoskeletal networks

F.C. MacKintosh

ABSTRACT: Most plant and animal cells possess a complex structure of filamentous proteins and associated proteins and enzymes for bundling, cross-linking, and active force generation. This *cytoskeleton* is largely responsible for cell elasticity and mechanical stability. It can also play a key role in cell locomotion. Over the last few years, the single-molecule micromechanics of many of the important constituents of the cytoskeleton have been studied in great detail by biophysical techniques such as high-resolution microscopy, scanning force microscopy, and optical tweezers. At the same time, numerous *in vitro* experiments aimed at understanding some of the unique mechanical and dynamic properties of solutions and networks of cytoskeletal filaments have been performed. In parallel with these experiments, theoretical models have emerged that have both served to explain many of the essential material properties of these networks, as well as to motivate quantitative experiments to determine, for example concentration dependence of shear moduli and the effects of cross-links. This chapter is devoted to theoretical models of the cytoskeleton based on polymer physics at both the level of single protein filaments and the level of solutions and networks of cross-linked or entangled filaments. We begin with a derivation of the static and dynamic properties of single cytoskeletal filaments. We then proceed to build up models of solutions and cross-linked gels of cytoskeletal filaments and we discuss the comparison of these models with a variety of experiments on *in vitro* model systems.

Introduction

Understanding the mechanical properties of cells and even whole tissues continues to pose significant challenges. Cells experience a variety of external stresses and forces, and they exert forces on their surroundings – for instance, in cell locomotion. The mechanical interaction of cells with their surroundings depends on structures such as cell membranes and complex networks of filamentous proteins. Although these cellular components have been known for many years, important outstanding problems remain concerning the origins and regulation of cell mechanical properties (Pollard and Cooper, 1986; Alberts et al., 1994; Boal, 2002). These mechanical factors determine how a cell maintains and modifies its shape, how it moves, and even how cells adhere to one another. Mechanical stimulus of cells can also result in changes in gene expression.

Cells exhibit rich composite structures ranging from the nanometer to the micrometer scale. These structures combine soft membranes and rather rigid filamentous

Polymer-based models of cytoskeletal networks

153

proteins or biopolymers, among other components. Most plant and animal cells, in fact, possess a complex network structure of biopolymers and associated proteins and enzymes for bundling, cross-linking, and active force generation. This *cytoskeleton* is often the principal determinant of cell elasticity and mechanical stability.

Over the last few years, the single-molecule properties of many of the important building blocks of the cytoskeleton have been studied in great detail by biophysical techniques such as high-resolution microscopy, scanning force microscopy, and optical tweezers. At the same time, numerous *in vitro* experiments have aimed to understand some of the unique mechanical and dynamic properties of solutions and networks of cytoskeletal filaments. In parallel with these experiments, theoretical models have emerged that have served both to explain many of the essential material properties of these networks, as well as to motivate quantitative experiments to determine the way material properties are regulated by, for example, cross-linking and bundling proteins. Here, we focus on recent theoretical modeling of cytoskeletal solutions and networks.

One of the principal components of the cytoskeleton, and even one of the most prevalent proteins in the cell, is actin. This exists in both monomeric or globular (G-actin) and polymeric or filamentary (F-actin) forms. Actin filaments can form a network of entangled, branched, and/or cross-linked filaments known as the actin cortex, which is frequently found near the periphery of cells. *In vivo*, this network is far from passive, with both active motion and (contractile) force generation during cell locomotion, and with a strong coupling to membrane proteins that appears to play a key role in the ability of cells to sense and respond to external stresses.

In order to understand these complex structures, quantitative models are needed for the structure, interactions, and mechanical response of networks such as the actin cortex. Unlike networks and gels of most synthetic polymers, however, these networks have been clearly shown to possess properties that cannot be modeled by existing polymer theories. These properties include rather large shear moduli (compared with synthetic polymers under similar conditions), strong signatures of nonlinear response (in which, for example, the shear modulus can increase by a full factor of ten or more under modest strains of only 10 percent or so) (Janmey et al., 1994), and unique dynamics. In a very close and active collaboration between theory and experiment over the past few years, a standard model of sorts for the material properties of *semiflexible* polymer networks has emerged, which can explain many of the observed properties of F-actin networks, at least *in vitro*. Central to these models has been the semiflexible nature of the constituent filaments, which is both a fundamental property of almost any filamentous protein, as well as a clear departure from conventional polymer physics, which has focused on flexible or rod-like limits. In contrast, biopolymers such as F-actin are nearly rigid on the scale of a micrometer, while at the same time showing significant thermal fluctuations on the cellular scale of a few microns.

This chapter begins with an introduction to models of single-filament response and dynamics, and in fact, spends most of its time on a detailed understanding of these single-filament properties. Because cytoskeletal filaments are the most important structural components in cells, a quantitative understanding of their mechanical response to bending, stretching, and compression is crucial for any model of the mechanics of networks of these filaments. We shall see how these fundamental

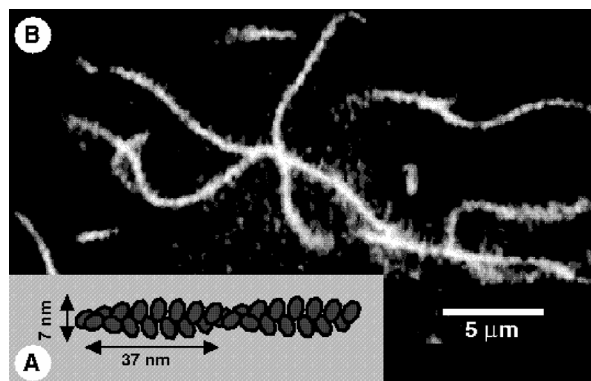


Fig. 8-1. Entangled solution of semiflexible actin filaments. (A) In physiological conditions, individual monomeric actin proteins (G-actin) polymerize to form double-stranded helical filaments known as F-actin. These filaments exhibit a polydisperse length distribution of up to $70\ \mu\text{m}$ in length. (B) A solution of $1.0\ \text{mg/ml}$ actin filaments, approximately 0.03% of which have been labeled with rhodamine-phalloidin in order to visualize them by fluorescence microscopy. The average distance ξ between chains in this figure is approximately $0.3\ \mu\text{m}$. (Reprinted with permission from MacKintosh F C, Käs J, and Janmey P A, *Physical Review Letters*, 75 4425 (1995). Copyright 1995 by the American Physical Society.

properties of the individual filaments can explain many of the properties of solutions and networks.

Single-filament properties

The biopolymers that make up the cytoskeleton consist of aggregates of large globular proteins that are bound together rather weakly, as compared with most synthetic, covalently bonded polymers. Nevertheless, they can be surprisingly strong. The most rigid of these are *microtubules*, which are hollow tube-like filaments that have a diameter of approximately 20 nm. The most basic aspect determining the mechanical behavior of cytoskeletal polymers on the cellular scale is their bending rigidity.

Even with this mechanical resistance to bending, however, cytoskeletal filaments can still exhibit significant thermally induced bending fluctuations because of Brownian motion in a liquid. Thus such filaments are said to be *semiflexible* or *worm-like*. This is illustrated in Fig. 8-1, showing fluorescently labeled F-actin filaments on the micrometer scale. The effect of the Brownian forces on the filament leads to increasingly contorted shapes over larger-length segments. The length at which significant bending fluctuations occur actually provides a simple yet quantitative characterization of the mechanical stiffness of such polymers. This thermal bending length, or *persistence length* ℓ_p , is defined in terms of the angular correlations (for example, of the local orientation along the polymer backbone), which decay exponentially with a characteristic length ℓ_p . In simple terms, however, this just says that a typical filament in thermal equilibrium in a liquid will appear rather straight over lengths that are short compared with this persistence length, while it will begin to exhibit a random, contorted shape only on longer-length scales. The persistence lengths of a few important biopolymers are given in Table 8-1, along with their approximate diameter and length.

Polymer-based models of cytoskeletal networks

Table 8-1. Persistence lengths and other parameters of various biopolymers (Howard, 2001; Gittes et al., 1993)

Type	Approximate diameter	Persistence length	Contour length
DNA	2 nm	50 nm	$\lesssim 1$ m
F-actin	7 nm	17 μm	$\lesssim 50$ μm
Microtubule	25 nm	~ 1 –5 mm	10s of μm

The worm-like chain model

Rigid polymers can be thought of as elastic rods, except on a small scale. The mechanical description of these is essentially the same as for a macroscopic rod with quantitative differences in parameters. The important role of thermal fluctuations, however, introduces a qualitative difference from the macroscopic case. Because the diameter of a filamentous protein is so much smaller than other length scales of interest – and especially the cellular scale – it is often sufficient to think of a filament as an idealized curve that resists bending. This is the essence of the so-called worm-like chain model. This can be described by an energy of the form,

$$H_{\text{bend}} = \frac{\kappa}{2} \int ds \left| \frac{\partial \vec{t}}{\partial s} \right|^2, \quad (8.1)$$

where κ is the *bending modulus* and \vec{t} is a (unit) tangent vector along the chain. The variation (derivative) of the tangent is a measure of curvature, which appears here quadratically because it is assumed that there is no preferred direction of curvature. Here, the chain position $\vec{r}(s)$ is described in terms of a coordinate s corresponding to the length along the chain backbone. Hence, the tangent vector

$$\vec{t} = \frac{\partial \vec{r}}{\partial s}.$$

These quantities are illustrated in Fig. 8-2.

The bending modulus κ has units of energy times length. A natural energy scale for a rod subject to Brownian fluctuations is kT , where T is the temperature and k is Boltzmann's constant. This is the typical kinetic energy of a molecule or particle. The persistence length described above is simply given by $\ell_p = \kappa/(kT)$, because the fluctuations tend to decrease with stiffness κ and increase with temperature. As noted, this is the typical length scale over which the polymer forgets its orientation, due to the constant Brownian forces it experiences in a medium at finite temperature.

More precisely, for a homogeneous rod of diameter $2a$ consisting of a homogeneous elastic material, the bending modulus should be proportional to the Young's modulus E . The Young's modulus, or the stiffness of the material, has units of energy per volume. Thus, on dimensional grounds, we expect that $\kappa \sim E a^4$. In fact (Landau and Lifshitz 1986),

$$\kappa = \frac{\pi}{4} E a^4.$$

The prefactor in front of $E a^4$ depends on the geometry of the rod (in other words, its cross-section). The factor $\pi a^4/4$ is for a solid rod of radius a . For a hollow tube, such

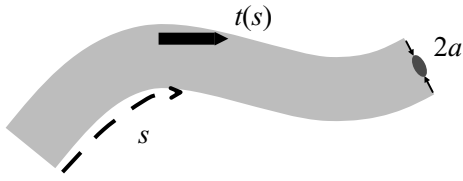


Fig. 8-2. A filamentous protein can be regarded as an elastic rod of radius a . Provided the length of the rod is very long compared with the monomeric dimension a , and that the rigidity is high (specifically, the persistence length $\ell_p \gg a$), this can be treated as an abstract line or curve, characterized by the length s along its backbone. A unit vector \vec{t} tangent to the filament defines the local orientation of the filament. Curvature is present when this orientation varies with s . For bending in a plane, it is sufficient to consider the angle $\theta(s)$ that the filament makes with respect to some fixed axis. The curvature is then $\partial\theta/\partial s$.

as one might use to model a microtubule, the prefactor would be different, but still of order a^4 , where a is the (outer) radius. This is often expressed as $\kappa = EI$, where I is the moment of inertia of the cross-section (Howard, 2001).

In general, for bending in 3D, there are two independent directions for deflections of the rod or polymer transverse to its local axis. It is often instructive, however, to consider a simpler case of a single transverse degree of freedom, in other words, motion confined to a plane, as illustrated by Fig. 8-2. Here, the integrand in Eq. 8.1 becomes $(\partial\theta/\partial s)^2$, where $\theta(s)$ is simply the local angle that the chain axis makes at point s , relative to any fixed axis. Using basic principles of statistical mechanics (Grosberg and Khokhlov, 1994), one can calculate the thermal average angular correlation between distant points along the chain, for which

$$\langle \cos[\theta(s) - \theta(s')] \rangle \simeq \langle \cos(\Delta\theta) \rangle^{|s-s'|/\Delta s} \simeq e^{-|s-s'|/2\ell_p}. \quad (8.2)$$

As noted at the outset, so far this is all for motion confined to a plane. In three dimensions, there is another direction perpendicular to the plane that the filament can move in. This increases the rate of decay of the angular correlations by a factor of two relative to the result above:

$$\langle \vec{t}(s) \cdot \vec{t}(s') \rangle = e^{-|s-s'|/\ell_p}, \quad (8.3)$$

where ℓ_p is the same persistence length defined above. This is a general definition of the persistence length, which also provides a purely *geometric* measure of the *mechanical* stiffness of the rod, provided that it is in equilibrium at temperature T . In principle, this means that one can measure the stiffness of a biopolymer by simply examining its bending fluctuations in a microscope. In practice, however, it is usually better to measure the amplitudes of a number of different bending modes (that is, different wavelengths) in order to ensure that thermal equilibrium is established (Gittes et al., 1993).

Force-extension of single chains

In order to understand how a network of filaments responds to mechanical loading, we need to understand at least two things: the way a single filament responds to stress; and the way in which the individual filaments are connected or otherwise interact with each

other. We address the single-filament properties here, and reserve the characterization of the way filaments interact for later.

A single filament can respond to forces in at least two ways. It can respond to both transverse and longitudinal forces by either bending or stretching/compressing. On length scales shorter than the persistence length, bending can be described in mechanical terms, as for elastic rods. By contrast, stretching and compression can involve both a purely elastic or mechanical response (again, as in the stretching, compression, or even buckling of macroscopic elastic rods), as well as an entropic response. The latter comes from the thermal fluctuations of the filament. Perhaps surprisingly, as will be shown, the longitudinal response can be dominated by entropy even on length scales small compared with the persistence length. Thus, it is incorrect to think of a filament as truly rod-like, even on length scales short compared with ℓ_p .

The longitudinal single-filament response is often described in terms of a so-called force-extension relationship. Here, the force required to extend the filament is measured or calculated in terms of the degree of extension along a line. At any finite temperature, there is a resistance to such extension due to the presence of thermal fluctuations that make the polymer deviate from a straight conformation. This has been the basis of mechanical studies, for example, of long DNA (Bustamante et al., 1994). In the limit of large persistence length, this can be calculated as follows (MacKintosh et al., 1995).

We consider a filament segment of length ℓ that is short compared with the persistence length ℓ_p . It is then nearly straight, with small transverse fluctuations. We let the x -axis define the average orientation of the chain segment, and let u and v represent the two independent transverse degrees of freedom. These can then be thought of as functions of x and time t in general. For simplicity, we shall mostly consider just one of these coordinates, $u(x, t)$. The bending energy is then

$$H_{\text{bend}} = \frac{\kappa}{2} \int dx \left(\frac{\partial^2 u}{\partial x^2} \right)^2 = \frac{\ell}{4} \sum_q \kappa q^4 u_q^2, \quad (8.4)$$

where we have represented $u(x)$ by a Fourier series

$$u(x, t) = \sum_q u_q \sin(qx). \quad (8.5)$$

As illustrated in Fig. 8-3, the local orientation of the filament is given by the slope $\partial u / \partial x$, while the local curvature is given by the second derivative $\partial^2 u / \partial x^2$. Such a description is appropriate for the case of a nearly straight filament with fixed boundary conditions $u = 0$ at the ends, $x = 0, \ell$. For this case, the wave vectors $q = n\pi/\ell$, where $n = 1, 2, 3, \dots$

We assume that the chain has no compliance in its contour length, in other words, that the total arc length $\int ds$ is unchanged by the fluctuations. As illustrated in Fig. 8-3, for a nearly straight filament, the arc length ds of a short segment is approximately given by $\sqrt{(dx)^2 + (du)^2} = dx \sqrt{1 + |\partial u / \partial x|^2}$. The contraction of the chain relative to its full contour length in the presence of thermal fluctuations in u is then

$$\Delta \ell = \int dx \left(\sqrt{1 + |\partial u / \partial x|^2} - 1 \right) \simeq \frac{1}{2} \int dx |\partial u / \partial x|^2. \quad (8.6)$$



Fig. 8-3. From one fixed end, a filament tends to wander in a way that can be characterized by $u(x)$, the transverse displacement from an initial straight line (dashed). If the arc length of the filament is unchanged, then the transverse thermal fluctuations result in a contraction of the end-to-end distance, which is denoted by $\Delta\ell$. In fact, this contraction is actually distributed about a thermal average value $\langle\Delta\ell\rangle$. The mean-square (longitudinal) fluctuations about this average are denoted by $\langle\delta\ell^2\rangle$, while the mean-square lateral fluctuations (that is, with respect to the dashed line) are denoted by $\langle u^2\rangle$.

The integration here is actually over the projected length of the chain. But, to leading (quadratic) order in the transverse displacements, we make no distinction between projected and contour lengths here, and above in H_{bend} .

Thus, the contraction

$$\Delta\ell = \frac{\ell}{4} \sum_q q^2 u_q^2. \quad (8.7)$$

Conjugate to this variable is the tension τ in the chain. Thus, we consider the effective energy

$$H = \frac{1}{2} \int dx \left[\kappa \left(\frac{\partial^2 u}{\partial x^2} \right)^2 + \tau \left(\frac{\partial u}{\partial x} \right)^2 \right] = \frac{\ell}{4} \sum_q (\kappa q^4 + \tau q^2) u_q^2. \quad (8.8)$$

Under a constant tension τ , therefore, the equilibrium amplitudes u_q must satisfy

$$\langle |u_q|^2 \rangle = \frac{2kT}{\ell (\kappa q^4 + \tau q^2)}, \quad (8.9)$$

and the contraction

$$\langle \Delta\ell \rangle = kT \sum_q \frac{1}{(\kappa q^2 + \tau)}. \quad (8.10)$$

There are, of course, two transverse degrees of freedom, and so this last answer incorporates a factor of two appropriate for a chain fluctuating in 3D.

Semiflexible filaments exhibit a strong suppression of bending fluctuations for modes of wavelength less than the persistence length ℓ_p . More precisely, as we see from Eq. 8.9 the mean-square amplitude of shorter wavelength modes are increasingly suppressed as the fourth power of the wavelength. This has important consequences for many of the thermal properties of such filaments. In particular, it means that the longest unconstrained wavelengths tend to be dominant in most cases. This allows us, for instance, to anticipate the scaling form of the end-to-end contraction $\Delta\ell$ between points separated by arc length ℓ in the absence of an applied tension. We note that it is a length and it must vary inversely with stiffness κ and must increase with temperature. Thus, as the dominant mode of fluctuations is that of the maximum wavelength, ℓ , we expect the contraction to be of the form $\langle \Delta\ell \rangle_0 \sim \ell^2 / \ell_p$. More precisely, for $\tau = 0$,

$$\langle \Delta\ell \rangle_0 = \frac{kT\ell^2}{\kappa\pi^2} \sum_{n=1}^{\infty} \frac{1}{n^2} = \frac{\ell^2}{6\ell_p}. \quad (8.11)$$

Polymer-based models of cytoskeletal networks

159

Similar scaling arguments to those above lead us to expect that the typical transverse amplitude of a segment of length ℓ is approximately given by

$$\langle u^2 \rangle \sim \frac{\ell^3}{\ell_p} \quad (8.12)$$

in the absence of applied tension. The precise coefficient for the mean-square amplitude of the midpoint between ends separated by ℓ (with vanishing deflection at the ends) is $1/24$.

For a finite tension τ , however, there is an extension of the chain (toward full extension) by an amount

$$\delta\ell = \langle \Delta\ell \rangle_0 - \langle \Delta\ell \rangle_\tau = \frac{kT\ell^2}{\kappa\pi^2} \sum_n \frac{\phi}{n^2(n^2 + \phi)}, \quad (8.13)$$

where $\phi = \tau\ell^2/(\kappa\pi^2)$ is a dimensionless force. The characteristic force $\kappa\pi^2/\ell^2$ that enters here is the critical force in the classical Euler buckling problem (Landau and Lifshitz, 1986). Thus, the force-extension curve can be found by inverting this relationship. In the linear regime, this becomes

$$\delta\ell = \frac{\ell^2}{\ell_p\pi^2} \phi \sum_n \frac{1}{n^4} = \frac{\ell^4}{90\ell_p\kappa} \tau, \quad (8.14)$$

that is, the effective spring constant for longitudinal extension of the chain segment is $90\kappa\ell_p/\ell^4$. The scaling form of this could also have been anticipated, based on very simple physical arguments similar to those above. In particular, given the expected dominance of the longest wavelength mode (ℓ), we expect that the end-to-end contraction scales as $\delta\ell \sim \int (\partial u/\partial x)^2 \sim u^2/\ell$. Thus, $\langle \delta\ell^2 \rangle \sim \ell^{-2} \langle u^4 \rangle \sim \ell^{-2} \langle u^2 \rangle^2 \sim \ell^4/\ell_p^2$, which is consistent with the effective (linear) spring constant derived above. The full nonlinear force-extension curve can be calculated numerically by inversion of the expression above. This is shown in Fig. 8-4. Here, one can see both the linear regime for small forces, with the effective spring constant given above, as well as a divergent force near full extension. In fact, the force diverges in a characteristic way, as the inverse square of the distance from full extension: $\tau \sim |\delta\ell - \Delta\ell|^{-2}$ (Fixman and Kovac, 1973).

We have calculated only the longitudinal response of semiflexible polymers that arises from their thermal fluctuations. It is also possible that such filaments will actually lengthen (in arc length) when pulled on. This we can think of as a *zero-temperature* or *purely mechanical* response. After all, we are treating semiflexible polymers as little bendable rods. To the extent that they behave as rigid rods, we might expect them to respond to longitudinal stresses by stretching as a rod. Based on the arguments above, it seems that the persistence length ℓ_p determines the length below which filaments behave like rods, and above which they behave like flexible polymers with significant thermal fluctuations. Perhaps surprisingly, however, even for semiflexible filament segments as short as $\ell \sim \sqrt[3]{a^2\ell_p}$, which is much shorter than the persistence length, their longitudinal response can be dominated by the entropic force-extension described above, that is, in which the response is due to transverse thermal fluctuations (Head et al., 2003b).

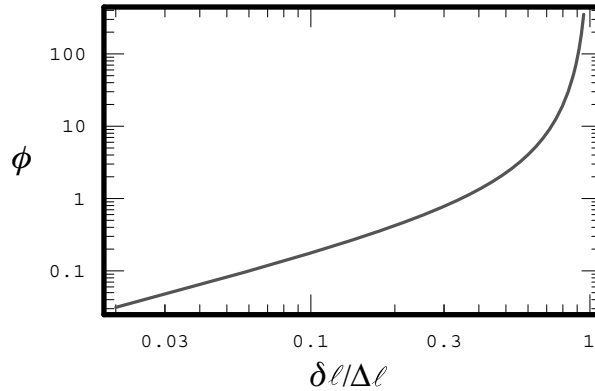


Fig. 8-4. The dimensionless force ϕ as a function of extension $\delta\ell$, relative to maximum extension $\Delta\ell$. For small extension, the response is linear.

Dynamics of single chains

The same Brownian forces that give rise to the bent shapes of filaments such as in Fig. 8.1 also govern the dynamics of these fluctuating filaments. Both the relaxation dynamics of bent filaments, as well as the dynamic fluctuations of individual chains exhibit rich behavior that can have important consequences even at the level of bulk solutions and networks. The principal dynamic modes come from the transverse motion, that is, the degrees of freedom u and v above. Thus, we must consider time dependence of these quantities. The transverse equation of motion of the chain can be found from H_{bend} above, together with the hydrodynamic drag of the filaments through the solvent. This is done via a Langevin equation describing the net force per unit length on the chain at position x ,

$$0 = -\zeta \frac{\partial}{\partial t} u(x, t) - \kappa \frac{\partial^4}{\partial x^4} u(x, t) + \xi_{\perp}(x, t), \quad (8.15)$$

which is, of course, zero within linearized, inertia-free (low Reynolds number) hydrodynamics that we assume here.

Here, the first term represents the hydrodynamic drag per unit length of the filament. We have assumed a constant transverse drag coefficient that is independent of wavelength. In fact, given that the actual drag per unit length on a rod of length L is $\zeta = 4\pi\eta/\ln(AL/a)$, where L/a is the aspect ratio of the rod, and A is a constant of order unity that depends on the precise geometry of the rod. For a filament fluctuating freely in solution, a weak logarithmic dependence on wavelength is thus expected. In practice, the presence of other chains in solution gives rise to an effective screening of the long-range hydrodynamics beyond a length of order the separation between chains, which can then be taken in place of L above. The second term in the Langevin equation above is the restoring force per unit length due to bending. It has been calculated from $-\delta H_{\text{bend}}/\delta u(x, t)$ with the help of integration by parts. Finally, we include a random force ξ_{\perp} that accounts for the motion of the surrounding fluid particles.

Polymer-based models of cytoskeletal networks

A simple force balance in the Langevin equation above leads us to conclude that the characteristic relaxation rate of a mode of wavevector q is (Farge and Maggs, 1993)

$$\omega(q) = \kappa q^4 / \zeta. \quad (8.16)$$

The fourth-order dependence of this rate on q is to be expected from the appearance of a single time derivative along with four spatial derivatives in Eq. 8.15. This relaxation rate determines, among other things, the correlation time for the fluctuating bending modes. Specifically, in the absence of an applied tension,

$$\langle u_q(t) u_q(0) \rangle = \frac{2kT}{\ell \kappa q^4} e^{-\omega(q)t}. \quad (8.17)$$

That the relaxation rate varies as the fourth power of the wavevector q has important consequences. For example, while the time it takes for an actin filament bending mode of wavelength $1 \mu\text{m}$ to relax is of order 10 ms, it takes about 100 s for a mode of wavelength $10 \mu\text{m}$. This has implications, for instance, for imaging of the thermal fluctuations of filaments, as is done in order to measure ℓ_p and the filament stiffness (Gittes et al., 1993). This is the basis, in fact, of most measurements to date of the stiffness of DNA, F-actin, and other biopolymers. Using Eq. 8.17, for instance, one can both confirm thermal equilibrium and determine ℓ_p by measuring the mean-square amplitude of the thermal modes of various wavelengths. However, in order both to resolve the various modes as well as to establish that they behave according to the thermal distribution, one must sample over times long compared with $1/\omega(q)$ for the longest wavelengths $\lambda \sim 1/q$. At the same time, one must be able to resolve fast motion on times of order $1/\omega(q)$ for the shortest wavelengths. Given the strong dependence of these relaxation times on the corresponding wavelengths, for instance, a range of order a factor of 10 in the wavelengths of the modes corresponds to a range of 10^4 in observation times.

Another way to look at the result of Eq. 8.16 is that a bending mode of wavelength λ relaxes (that is, fully explores its equilibrium conformations) in a time of order $\zeta \lambda^4 / \kappa$. Because it is also true that the longest (unconstrained) wavelength bending mode has by far the largest amplitude, and thus dominates the typical conformations of any filament (see Eqs. 8.10 and 8.17), we can see that in a time t , the *typical* or dominant mode that relaxes is one of wavelength $\ell_{\perp}(t) \sim (\kappa t / \zeta)^{1/4}$. As we have seen above in Eq. 8.12, the mean-square amplitude of transverse fluctuations increases with filament length ℓ as $\langle u^2 \rangle \sim \ell^3 / \ell_p$. Thus, in a time t , the expected mean-square transverse motion is given by (Farge and Maggs, 1993; Amblard et al., 1996)

$$\langle u^2(t) \rangle \sim (\ell_{\perp}(t))^3 / \ell_p \sim t^{3/4}, \quad (8.18)$$

because the typical and dominant mode contributing to the motion at time t is of wavelength $\ell_{\perp}(t)$. Equation 8.18 represents what can be called *subdiffusive* motion because the mean-square displacement grows less strongly with time than for diffusion or Brownian motion. Motion consistent with Eq. 8.18 has been observed in living cells, by tracking small particles attached to microtubules (Caspi et al., 2000). Thus, in some cases, the dynamics of cytoskeletal filaments in living cells appear to follow the expected motion for transverse equilibrium thermal fluctuations in viscous fluids.

The dynamics of longitudinal motion can be calculated similarly. It is found that the means-square amplitude of longitudinal fluctuations of filament of length ℓ are also governed by (Granek, 1997; Gittes and MacKintosh, 1998)

$$\langle \delta \ell(t)^2 \rangle \sim t^{3/4}, \quad (8.19)$$

where this mean-square amplitude is smaller than for the transverse motion by a factor of order ℓ/ℓ_p . Thus, both for the short-time fluctuations as well as for the static fluctuations of a filament segment of length ℓ , a filament end explores a disk-like region with longitudinal motion smaller than perpendicular motion by this factor. Although the amplitude of longitudinal motion is smaller than for transverse, the longitudinal motion of Eq. 8.19 can explain the observed high-frequency viscoelastic response of solutions and networks of biopolymers, as discussed below.

Solutions of semiflexible polymer

Because of their inherent rigidity, semiflexible polymers interact with each other in very different ways than flexible polymers would, for example, in solutions of the same concentration. In addition to the important characteristic lengths of the molecular dimension (say, the filament diameter $2a$), the material parameter ℓ_p , and the contour length of the chains, there is another important new length scale in a solution – the *mesh size*, or typical spacing between polymers in solution, ξ . This can be estimated as follows in terms of the molecular size a and the polymer volume fraction ϕ (Schmidt et al., 1989). In the limit that the persistence length ℓ_p is large compared with ξ , we can approximate the solution on the scale of the mesh as one of rigid rods. Hence, within a cubical volume of size ξ , there is of order one polymer segment of length ξ and cross-section a^2 , which corresponds to a volume fraction ϕ of order $(a^2\xi)/\xi^3$. Thus,

$$\xi \sim a/\sqrt{\phi}. \quad (8.20)$$

This mesh size, or spacing between filaments, does not completely characterize the way in which filaments interact, even sterically with each other. For a dilute solution of rigid rods, it is not hard to imagine that one can embed a long rigid rod rather far into such a solution before touching another filament. A true estimate of the distance between typical interactions (points of contact) of semiflexible polymers must account for their thermal fluctuations (Odijk, 1983). As we have seen, the transverse range of fluctuations δu a distance ℓ away from a fixed point grows according to $\delta u^2 \sim \ell^3/\ell_p$. Along this length, such a fluctuating filament explores a narrow cone-like volume of order $\ell\delta u^2$. An entanglement that leads to a constraint of the fluctuations of such a filament occurs when another filament crosses through this volume, in which case it will occupy a volume of order $a^2\delta u$, as $\delta u \ll \ell$. Thus, the volume fraction and the contour length ℓ between constraints are related by $\phi \sim a^2/(\ell\delta u)$. Taking the corresponding length as an entanglement length, and using the result above for $\delta u = \sqrt{\delta u^2}$, we find that

$$\ell_e \sim (a^4\ell_p)^{1/5} \phi^{-2/5}, \quad (8.21)$$

which is larger than the mesh size ξ in the semiflexible limit $\ell_p \gg \xi$.

These transverse entanglements, separated by a typical length ℓ_e , govern the elastic response of solutions, in a way first outlined in Isambert and Maggs (1996). A more complete discussion of the rheology of such solutions can be found in Morse (1998b) and Hinner et al. (1998). The basic result for the rubber-like plateau shear modulus for such solutions can be obtained by noting that the number density of entropic constraints (entanglements) is thus $n\ell/\ell_c \sim 1/(\xi^2\ell_e)$, where $n = \phi/(a^2\ell)$ is the number density of chains of contour length ℓ . In the absence of other energetic contributions to the modulus, the entropy associated with these constraints results in a shear modulus of order $G \sim kT/(\xi^2\ell_e) \sim \phi^{7/5}$. This has been well established in experiments such as those of Hinner et al. (1998).

With increasing frequency, or for short times, the macroscopic shear response of solutions is expected to show the underlying dynamics of individual filaments. One of the main signatures of the frequency response of polymer solutions in general is an increase in the shear modulus with increasing frequency. This is simply because the individual filaments are not able to fully relax or explore their conformations on short times. In practice, for high molecular weight F-actin solutions of approximately 1 mg/ml, this frequency dependence is seen for frequencies above a few Hertz. Initial experiments measuring this response by imaging the dynamics of small probe particles have shown that the shear modulus increases as $G(\omega) \sim \omega^{3/4}$ (Gittes et al., 1997; Schnurr et al., 1997), which has since been confirmed in other experiments and by other techniques (for example, Gisler and Weitz, 1999).

If, as noted above, this increase in stiffness with frequency is due to the fact that filaments are not able to fully fluctuate on the correspondingly shorter times, then we should be able to understand this more quantitatively in terms of the dynamics described in the previous section. In particular, this behavior can be understood in terms of the longitudinal dynamics of single filaments (Morse, 1998a; Gittes and MacKintosh, 1998). Much as the static longitudinal fluctuations $\langle \delta\ell^2 \rangle \sim \ell^4/\ell_p^2$ correspond to an effective longitudinal spring constant $\sim kT\ell_p^2/\ell^4$, the time-dependent longitudinal fluctuations shown above in Eq. 8.19 correspond to a time- or frequency-dependent compliance or stiffness, in which the effective spring constant increases with increasing frequency. This is because, on shorter time scales, fewer bending modes can relax, which makes the filament less compliant. Accounting for the random orientations of filaments in solution results in a frequency-dependent shear modulus

$$G(\omega) = \frac{1}{15}\rho\kappa\ell_p(-2i\zeta/\kappa)^{3/4}\omega^{3/4} - i\omega\eta, \quad (8.22)$$

where ρ is the polymer concentration measured in length per unit volume.

Network elasticity

In a living cell, there are many different specialized proteins for binding, bundling, and otherwise modifying the network of filamentous proteins. Many tens of actin-associated proteins alone have been identified and studied. Not only is it important to understand the mechanical roles of, for example, cross-linking proteins, but as we shall see, these can have a much more dramatic effect on the network properties than is the case for flexible polymer solutions and networks.

The introduction of cross-linking agents into a solution of semiflexible filaments introduces yet another important and distinct length scale, which we shall call the cross-link distance ℓ_c . As we have just seen, in the limit that $\ell_p \gg \xi$, individual filaments may interact with each other only infrequently. That is to say, in contrast with flexible polymers, the distance between interactions of one polymer with its neighbors (ℓ_e in the case of solutions) may be much larger than the typical spacing between polymers. Thus, if there are biochemical cross-links between filaments, these may result in significant variation of network properties even when ℓ_c is larger than ξ .

Given a network of filaments connected to each other by cross-links spaced an average distance ℓ_c apart along each filament, the response of the network to macroscopic strains and stresses may involve two distinct single-filament responses: (1) bending of filaments; and (2) stretching/compression of filaments. Models based on both of these effects have been proposed and analyzed. Bending-dominated behavior has been suggested both for ordered (Satcher and Dewey, 1996) and disordered (Kroy and Frey, 1996) networks. That individual filaments bend under network strain is perhaps not surprising, unless one thinks of the case of uniform shear. In this case, only rotation and stretching or compression of individual rod-like filaments are possible. This is the basis of so-called *affine* network models (MacKintosh et al., 1995), in which the macroscopic strain falls uniformly across the sample. In contrast, bending of constituents involves *non-affine* deformations, in which the state of strain varies from one region to another within the sample.

We shall focus mostly on random networks, such as those studied *in vitro*. It has recently been shown (Head et al., 2003a; Wilhelm and Frey, 2003; Head et al., 2003b) that which of the *affine* or *non-affine* behaviors is expected depends, for instance, on filament length and cross-link concentration. Non-affine behavior is expected either at low concentrations or for short filaments, while the deformation is increasingly affine at high concentration or for long filaments. For the first of these responses, the network shear modulus (*Non-Affine*) is expected to be of the form

$$G_{\text{NA}} \sim \kappa/\xi^4 \sim \phi^2 \quad (8.23)$$

when the density of cross-links is high (Kroy and Frey 1996). This quadratic dependence on filament concentration c is also predicted for more ordered networks (Satcher and Dewey 1996).

For affine deformations, the modulus can be estimated using the effective single-filament longitudinal spring constant for a filament segment of length ℓ_c between cross-links, $\sim \kappa \ell_p / \ell_c^4$, as derived above. Given an area density of $1/\xi^2$ such chains passing through any shear plane (see Fig. 8-5), together with the effective tension of order $(\kappa \ell_p / \ell_c^3)\epsilon$, where ϵ is the strain, the shear modulus is expected to be

$$G_{\text{AT}} \sim \frac{\kappa \ell_p}{\xi^2 \ell_c^3}. \quad (8.24)$$

This shows that the shear modulus is expected to be strongly dependent on the density of cross-links. Recent experiments on *in vitro* model gels consisting of F-actin with permanent cross-links, for instance, have shown that the shear modulus can vary from less than 1 Pa to over 100 Pa at the same concentration of F-actin, by varying the cross-link concentration (Gardel et al., 2004).

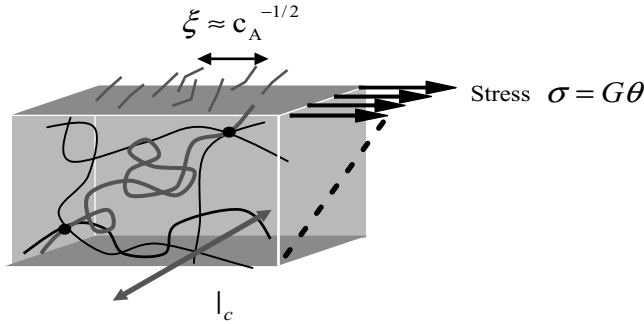


Fig. 8-5. The macroscopic shear stress σ depends on the mean tension in each filament, and on the area density of such filaments passing any plane. There are on average $1/\xi^2$ such filaments per unit area. This gives rise to the factor ξ^{-2} in both Eqs. 8.24 and 8.25. The macroscopic response can also depend strongly on the typical distance ℓ_c between cross-links, as discussed below.

In the preceding derivation we have assumed a thermal/entropic (Affine and Thermal) response of filaments to longitudinal forces. As we have seen, however, for shorter filament segments (that is, for small enough ℓ_c), one may expect a mechanical response characteristic of rigid rods that can stretch and compress (with a modulus μ). This would lead to a different expression (Affine, Mechanical) for the shear modulus

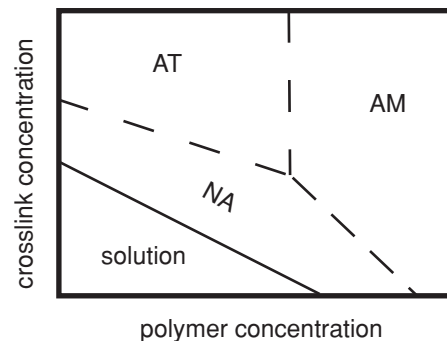
$$G_{AM} \sim \frac{\mu}{\xi^2} \sim \phi, \tag{8.25}$$

which is proportional to concentration. The expectations for the various mechanical regimes is shown in Fig. 8.6 (Head et al., 2003b).

Nonlinear response

In contrast with most polymeric materials (such as gels and rubber), most biological materials, from the cells to whole tissues, stiffen as they are strained even by a few percent. This nonlinear behavior is also quite well established by *in vitro* studies of a wide range of biopolymers, including networks composed of F-actin, collagen, fibrin, and a variety of intermediate filaments (Janmey et al., 1994; Storm et al., 2005). In particular, these networks have been shown to exhibit approximately ten-fold

Fig. 8-6. A sketch of the expected diagram showing the various elastic regimes in terms of cross-link density and polymer concentration. The solid line represents the rigidity percolation transition where rigidity first develops from a solution at a macroscopic level. The other, dashed lines indicate crossovers (not thermodynamic transitions). NA indicates the non-affine regime, while AT and AM refer to affine thermal (or entropic) and mechanical, respectively.



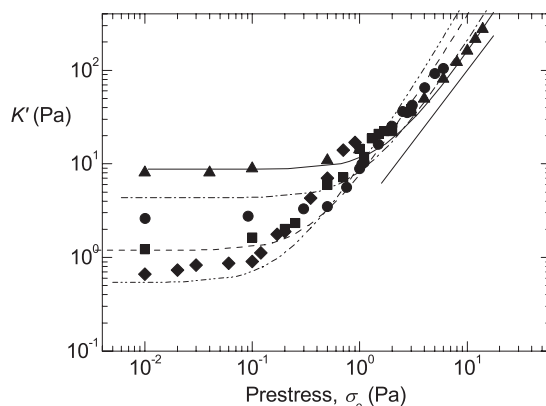


Fig. 8-7. The differential modulus $K' = d\sigma/d\gamma$ describes the increase in the stress σ with strain γ in the nonlinear regime. This was measured for cross-linked actin networks by small-amplitude oscillations at low frequency, corresponding to a nearly purely elastic response, after applying a constant prestress σ_0 . This was measured for four different concentrations represented by the various symbols. For small prestress σ_0 , the differential modulus K' is nearly constant, corresponding to a linear response for the network. With increasing σ_0 , the network stiffens, in a way consistent with theoretical predictions (MacKintosh et al., 1995; Gardel et al., 2004), as illustrated by the various theoretical curves. Specifically, it is expected that in the strongly nonlinear regime, the stiffening increases according to the straight line, corresponding to $d\sigma/d\gamma \sim \sigma^{3/2}$. Data taken from Gardel et al., 2004.

stiffening under strain. Thus these materials are compliant, while being able to withstand a wide range of shear stresses.

This strain-stiffening behavior can be understood in simple terms by looking at the characteristic force-extension behavior of individual semiflexible filaments, as described above. As can be seen in Fig. 8-4, for small extensions or strains, there is a linear increase in the force. As the strain increases, however, the force is seen to grow more rapidly. In fact, in the absence of any compliance in the arc length of the filament, the force strictly diverges at a finite extension. This suggests that for a network, the macroscopic stress should diverge, while in the presence of high stress, the macroscopic shear strain is bounded and ceases to increase. In other words, after being compliant at low stress, such a material will be seen to stop responding, even under high applied stress.

This can be made more quantitative by calculating the macroscopic shear stress of a strained network, including random orientations of the constituent filaments (MacKintosh et al., 1995; Kroy and Frey, 1996; Gardel et al., 2004; Storm et al., 2005). Specifically, for a given shear strain γ , the tension in a filament segment of length ℓ_c is calculated, based on the force-extension relation above. This is done within the (affine) approximation of uniform strain, in which the microscopic strain on any such filament segment is determined precisely by the macroscopic strain and the filament's orientation with respect to the shear. The contribution of such a filament's tension to the macroscopic stress, in other words, in a horizontal plane in Fig. 8.5, also depends on its orientation in space. Finally, the concentration or number density of such filaments crossing this horizontal plane is a function of the overall polymer concentration, and the filament orientation.

Polymer-based models of cytoskeletal networks

167

The full nonlinear shear stress is calculated as a function of γ , the polymer concentration, and ℓ_c , by adding all such contributions from all (assumed random) orientations of filaments. This can then be compared with macroscopic rheological studies of cross-linked networks, such as done recently by Gardel et al. (2004). These experiments measured the differential modulus, $d\sigma/d\gamma$ versus applied stress σ , and found good agreement with the predicted increase in this modulus with increasing stress (Fig. 8-7). In particular, given the quadratic divergence of the single-filament tension shown above (Fixman and Kovac, 1973), this modulus is expected to increase as $d\sigma/d\gamma \sim \sigma^{3/2}$, which is consistent with the experiments by Gardel et al. (2004). This provides a strong test of the underlying mechanism of network elasticity.

In addition to good agreement between theory and experiment for densely cross-linked networks, these experiments have also shown evidence of a lack of strain-stiffening behavior of these networks at lower concentrations (of polymer or cross-links), which may provide evidence for a non-affine regime of network response described above.

Discussion

Cytoskeletal filaments play key mechanical roles in the cell, either individually (for example, as paths for motor proteins) or in collective structures such as networks. The latter may involve many associated proteins for cross-linking, bundling, or coupling the cytoskeleton to other cellular structures like membranes. Our knowledge of the cytoskeleton has improved in recent years through the development of new experimental techniques, such as in visualization and micromechanical probes in living cells. At the same time, combined experimental and theoretical progress on *in vitro* model systems has provided fundamental insights into the possible mechanical mechanisms of cellular response.

In addition to their role in cells, cytoskeletal filaments have also proven remarkable model systems for the study of semiflexible polymers. Their size alone makes it possible to visualize individual filaments directly. They are also unique in the extreme separation of two important lengths, the persistence length ℓ_p and the size of a single monomer. In the case of F-actin, ℓ_p is more than a thousand times the size of a single monomer. This makes for not only quantitative but also qualitative differences from most synthetic polymers. We have seen, for instance, that the way in which semiflexible polymers entangle is very different. This makes for a surprising variation of the stiffness of these networks with only changes in the density of cross-links, even at the same concentration.

In spite of the molecular complexity of filamentous proteins as compared with conventional polymers, a quantitative understanding of the properties of single filaments provides a quantitative basis for modeling solutions and networks of filaments. In fact, the macroscopic response of cytoskeletal networks quite directly reflects, for example, the underlying dynamics of an individual semiflexible chain fluctuating in its Brownian environment. This can be seen, for instance in the measured dynamics of microtubules in cells (Caspi et al., 2000).

In developing our current understanding of cytoskeletal networks, a crucial role has been played by *in vitro* model systems, such as the one in Fig. 8-1. Major challenges,

however, remain for understanding the cytoskeleton of living cells. In the cell, the cytoskeleton is hardly a passive network. Among other differences from the model systems studied to date is the presence of active contractile or force-generating elements such as motors that work in concert with filamentous proteins. Nevertheless, *in vitro* models may soon permit a systematic and quantitative study of various actin-associated proteins for cross-linking and bundling (Gardel et al., 2004), and even contractile elements such as motors.

References

- Alberts B, et al., 1994, *Molecular Biology of the Cell*, 3rd edn. (Garland Press, New York).
- Amblard F, Maggs A C, Yurke B, Pargellis A N, and Leibler S, 1996, Subdiffusion and anomalous local viscoelasticity in actin networks, *Phys. Rev. Lett.*, **77** 4470–4473.
- Boal D, 2002, *Mechanics of the Cell* (Cambridge University Press, Cambridge).
- Bustamante C, Marko J F, Siggia E D, and Smith S, 1994, Entropic elasticity of lambda-phage DNA, *Science*, **265** 1599–1600.
- Caspi A, Granek R, and Elbaum M, 2000, Enhanced diffusion in active intracellular transport, *Phys. Rev. Lett.*, **85** 5655.
- Farge E and Maggs A C, 1993, Dynamic scattering from semiflexible polymers. *Macromolecules*, **26** 5041–5044.
- Fixman M and Kovac J, 1973, Polymer conformational statistics. III. Modified Gaussian models of stiff chains, *J. Chem. Phys.*, **58** 1564.
- Gardel M L, Shin J H, MacKintosh F C, Mahadevan L, Matsudaira P, and Weitz D A, 2004, Elastic behavior of cross-linked and bundled actin networks, *Science*, **304** 1301.
- Gisler T and Weitz D A, 1999, Scaling of the microrheology of semidilute F-actin solutions, *Phys. Rev. Lett.*, **82** 1606.
- Gittes F, Mickey B, Nettleton J, and Howard J, 1993, Flexural rigidity of microtubules and actin filaments measured from thermal fluctuations in shape. *J. Cell Biol.*, **120** 923–934.
- Gittes F, Schnurr B, Olmsted, P D, MacKintosh, F C, and Schmidt, C F, 1997, Microscopic viscoelasticity: Shear moduli of soft materials determined from thermal fluctuations, *Phys. Rev. Lett.*, **79** 3286–3289.
- Gittes F and MacKintosh F C, 1998, Dynamic shear modulus of a semiflexible polymer network, *Phys. Rev. E.*, **58** R1241–1244.
- Granek R, 1997, From semi-flexible polymers to membranes: Anomalous diffusion and reptation, *J. Phys. II (France)*, **7** 1761.
- Grosberg A Y and Khokhlov A R, 1994, *Statistical Physics of Macromolecules* (American Institute of Physics Press, New York).
- Head D A, Levine A J, and MacKintosh F C, 2003a, Deformation of cross-linked semiflexible polymer networks, *Phys. Rev. Lett.*, **91** 108102.
- Head D A, Levine A J, and MacKintosh F C, 2003b, Distinct regimes of elastic response and deformation modes of cross-linked cytoskeletal and semiflexible polymer networks, *Phys. Rev. E.*, **68** 061907.
- Hinner B, Tempel M, Sackmann E, Kroy K, and Frey E, 1998, Entanglement, elasticity, and viscous relaxation of actin solutions *Phys. Rev. Lett.*, **81** 2614.
- Howard J, 2001, *Mechanics of Motor Proteins and the Cytoskeleton* (Sinauer Press, Sunderland, MA).
- Isambert H, and Maggs A C, 1996, Dynamics and Rheology of actin solutions, *Macromolecules* **29** 1036–1040.
- Janmey P A, Hvidt S, Käs J, Lerche D, Maggs, A C, Sackmann E, Schliwa M, and Stossel T P, 1994, The mechanical properties of actin gels. Elastic modulus and filament motions, *J. Biol. Chem.*, **269**, 32503–32513.
- Kroy K and Frey E, 1996, Force-extension relation and plateau modulus for wormlike chains, *Phys. Rev. Lett.*, **77** 306–309.

Polymer-based models of cytoskeletal networks

169

- Landau L D, and Lifshitz E M, 1986, *Theory of Elasticity* (Pergamon Press, Oxford).
- MacKintosh F C, Käs J, and Janmey P A, 1995, Elasticity of semiflexible biopolymer networks, *Phys. Rev. Lett.*, **75** 4425.
- Morse D C, 1998a, Viscoelasticity of tightly entangled solutions of semiflexible polymers, *Phys. Rev. E.*, **58** R1237.
- Morse D C, 1998b, Viscoelasticity of concentrated isotropic solutions of semiflexible polymers. 2. Linear response, *Macromolecules*, **31** 7044.
- Odijk T, 1983, The statistic and dynamics of confined or entangled stiff polymers, *Macromolecules*, **16** 1340.
- Pasquali M, Shankar V, and Morse D C, 2001, Viscoelasticity of dilute solutions of semiflexible polymers, *Phys. Rev. E.*, **64** 020802(R).
- Pollard T D and Cooper J A, 1986, Actin and actin-binding proteins. A critical evaluation of mechanisms and functions, *Ann. Rev. Biochem.*, **55** 987.
- Satcher R L and Dewey C F, 1996, Theoretical estimates of mechanical properties of the endothelial cell cytoskeleton, *Biophys. J.*, **71** 109–11.
- Schmidt C F, Baermann M, Isenberg G, and Sackmann E, 1989, Chain dynamics, mesh size, and diffusive transport in networks of polymerized actin - a quasielastic light-scattering and microfluorescence study, *Macromolecules*, **22**, 3638–3649.
- Schnurr B, Gittes F, Olmsted P D, MacKintosh F C, and Schmidt C F, 1997, Determining microscopic viscoelasticity in flexible and semiflexible polymer networks from thermal fluctuations, *Macromolecules*, **30** 7781–7792.
- Storm C, Pastore J J, MacKintosh F C, Lubensky T C, and Janmey P J, 2005, Nonlinear elasticity in biological gels, *Nature*, **435** 191.
- Wilhelm J and Frey E, 2003, *Phys. Rev. Lett.*, **91** 108103.